HEFAT2012
9th International Conference on Heat Transfer, Fluid Mechanics and Thermodynamics
16 – 18 July 2012
Malta

A FRAMEWORK FOR THE ANALYSIS OF THERMAL LOSSES IN RECIPROCATING COMPRESSORS AND EXPANDERS

Mathie R., Markides C.N.* and White A.J.
*Author for correspondence
Department of Chemical Engineering,
Imperial College London,
London, SW7 2AZ,
United Kingdom.
E-mail: c.markides@imperial.ac.uk

ABSTRACT

The establishment of a reliable methodology for the design of a host of practical thermal and thermodynamic systems demands the development of a framework that can accurately predict their performance by accounting formally for the underlying unsteady and conjugate heat transfer processes that are undergone as part of their operation. The purpose of this paper is to present a framework that includes such a description and to show results from its application to the characterisation of a reciprocating compression and expansion process. Specifically, an unsteady and conjugate heat transfer model is proposed that solves the one-dimensional unsteady heat conduction equation in the solid simultaneously with the first law in the gas phase, with an imposed heat transfer coefficient taken from relevant experimental studies in the literature. This model is applied to the study of thermal losses in gas springs. Beyond the explicit inclusion of conjugate heat transfer, the present model goes beyond previous efforts by considering the case of imposed volumetric compression and by allowing the resulting gas pressure to vary accordingly.

Notable effects of the solid walls of the gas spring are revealed, with worst case thermodynamic cycle losses of up to 14% (relative to equivalent adiabatic and reversible processes) for cases in which unfavourable solid and gas materials are selected, and closer to 11% for more common material choices. The contribution of the solid towards these values, through the dimensionless thickness of the gas spring cylinder wall, is about 8% and 2%, respectively, showing a non-monotonic trend with the thermodynamic losses; increasing with increased solid thickness, reaching a maximum and then decreasing again. These results suggest strongly that, in designing high-efficiency reciprocating machines, the full conjugate and unsteady problem must be considered and that the role of the solid in determining the performance of the cycle undergone by the gas cannot, in general, be neglected.

INTRODUCTION

Unsteady and Conjugate Heat Transfer

Numerous engines, thermal-fluid devices and other systems are capable of utilising clean and renewable energy sources such as solar, geothermal and waste heat, which is expected to render them increasingly relevant in domestic, as well as industrial settings. A common feature of these systems concerns their interaction (externally) with inherently time-varying fluid and heat streams (e.g., flow rates, pressures, temperatures), and/or the occurrence (internally) of naturally time-varying thermodynamic processes during operation, even when the external conditions are steady. These interactions can readily give rise to *unsteady and conjugate* heat exchange, in which heat transfer occurs simultaneously by convection between the fluid streams and the internal surfaces of the relevant components and by conduction through the solid walls.

In many cases the unsteady (i.e., time-varying) heat transfer can take place simultaneously with pressure and density variations in the fluid, for example in thermoacoustic engines [1-3], dry free-liquid-piston (Fluidyne) engines [4-6] or two-phase thermofluidic oscillator equivalents [7-9], free-piston Stirling engines [10-12] and pulse-tubes [13-15], as well as in stand-alone compressors and expanders or when these units appear as components within larger systems. In some cases the conditions can give rise to *conjugate* heat transfer in the presence of the time-varying variations of pressure, density, and temperature. This is the subject of the present paper.

Rankine Cycle Expanders

Amongst other, compressors and expanders can be employed in Rankine Cycle engines, including organic (ORC)

equivalents [16], for power generation. In fact, an efficient and low-cost expander is a crucial component of any economically efficient ORC system. Typical breakdowns of the thermodynamic exergy destruction in the case of a basic and a regenerative ORC system reveal that, after the evaporator(s), the expander is the component associated with the largest performance penalty, with an exergetic loss of about 20% [17].

A variety of expanders are available and these are usually categorised as belonging to two main classes of machines:

1. Positive-displacement machines (also known as 'volume' type, such as pneumatic converters, or screw, scroll or reciprocating piston expanders); and,

2. Turbomachines (also 'velocity' or 'dynamic' type, such as axial or axial-flow turbine expanders).

Positive-displacement expanders are further classified according to the mechanism used for fluid flow (motion), into: (i) rotary expanders (including multi-vane or rotating piston expanders [18], screw or helical expanders [19] and scroll expanders [19-22]); and, (ii) reciprocating (or reciprocal) piston expanders [23]. Turbomachines include axial- and radial-flow (or centrifugal) turbine expanders (or turbo-expanders) [24].

Operational and specification data from expansion devices employed in over 2,000 Rankine engines were collected by Curran [25]. These data, that span power outputs from 0.1 to 1,120 kWe, reveal that low-speed expansion devices (<5,000 rpm) tend to be predominantly positive-displacement (e.g., reciprocating) machines producing power outputs of up to 10 kWe, while turbomachines on the other hand are adopted at higher speeds (>5,000 rpm) for meeting greater demands, with output shaft powers in excess of 10 kWe.

A second compilation of specification and performance information was employed by Balje [26] in order to identify the optimal geometries and maximum obtainable design efficiencies for different types of expander. The resulting compilation of performance characteristics indicates that at low speeds positive-displacement expanders offer superior performance (i.e., exhibit greater efficiencies) when compared to single-stage turbomachines. Rotary positive-displacement expanders achieve similar isentropic efficiencies η_{is} to single-stage turbines at specific diameters (and consequently sizes) that are only 1/4 to 1/3 of those required for single-stage turbo-expanders, while reciprocating positive-displacement expanders can achieve similar efficiencies at even lower speeds [26].

Piston Compressors and Expanders

As discussed above, positive-displacement machines offer the potential of higher efficiencies compared to turbomachines, especially in smaller-scale applications. In theoretical studies of reciprocating Joule/Brayton cycles [27,28], compression and expansion efficiencies in excess of 98% have been employed. Moss et al. [27] used isentropic efficiency values η_{is} of 97.5% for compression and 99.3% for expansion in the context of a reciprocating Joule/Brayton combined heat and power (CHP) plant, while White [28] based his study on theoretical values of 98% and 99% for the polytropic efficiency of reciprocating compressors and expanders as part of a reverse Joule/Brayton cycle heat pump for domestic applications. In both cases the authors concede that these figures are only estimates of minimum losses and not based upon direct measurement [28]. Where measurements do exist (see below) they suggest lower efficiencies, but in such cases it is likely that leakage flow and valve pressure losses (both of which have scope for reduction) are to a significant extent detrimentally affecting performance.

Nonetheless, for low-cost small-scale machines with medium to large leakage gaps manufactured with low precision, Table 1 (compiled from data found in Ref. [29]) suggests that reciprocating and rotary piston compressors and expanders also significantly outperform their scroll counterparts. Specifically, piston machines have indicated η_{ind} efficiencies in the range 85-91% for compression and 78-87% for expansion, and isentropic η_{is} in the range 72-76% for compression and 63-72% for expansion. In Ref. [29] it is also suggested that for even smaller leakage gap sizes of 5 μm, η_{ind} and η_{is} reach ~95% and ~90% for both compression and expansion, respectively.

Table 1 Positive-displacement compressor and expander indicated and isentropic efficiencies for a leakage gap size of 10-15 μm, taken from Ref. [29]

Machine	Type	η_{ind}	η_{is}
Compressor	Reciprocating piston	0.85-0.91	0.72-0.76
	Rotary piston	0.85-0.90	0.72-0.75
	Scroll	0.39-0.64	0.36-0.56
Expander	Reciprocating piston	0.81-0.87	0.66-0.72
	Rotary piston	0.78-0.84	0.63-0.69
	Scroll	0.47-0.75	0.32-0.69

Clearly, reciprocating and rotary piston compressors and expanders are of interest in the above mentioned applications. The present study focuses on reciprocating piston machines, however the results are transferable to rotary piston equivalents, as well as related engines and devices (e.g., [1-15]).

Irreversible Heat Transfer Losses

Performance losses in reciprocating engines, compressors and expanders arise from mechanical irreversibilities (i.e., mechanical friction, pressure drops through the intake and exhaust valves), but also from thermal irreversibilities (i.e., heat transfer between the fluid and walls of the device). In order to improve their efficiency it becomes essential to minimise all loss mechanisms. Valve losses may be minimised by a combination of careful valve timing, rapid opening and large open areas. Once mechanical losses have been minimised, thermal losses become the dominant loss mechanism. The present investigation focuses on this aspect of performance.

A performance loss in reciprocating systems arising as a consequence of unsteady heat transfer occurs even if the overall process is globally adiabatic (i.e., for zero time-mean heat transfer), since any heat exchange between the gas and cylinder walls is an inherently irreversible process. The exegetic loss due to the (zero-mean) heat transfer fluctuations arises as a consequence of the fact that heat from the fluid (gas, liquid or vapour) at a high temperature is temporarily stored in the solid walls which are at a lower temperature, and then returned (in its entirety) to the fluid at an even lower temperature. Although the *net fluctuating* heat loss is zero, an exergetic penalty is paid.

For this reason, beyond the steady (time-averaged) heat losses, it is important to be able to account for, characterise and predict accurately the time-varying heat exchange fluctuations between the fluid and solid. A further characteristic of interest concerns the timing (phase difference) of the heat transfer relative to the temperature fluctuations; in some systems the heat is lost and gained by the fluid at the wrong time in the cycle, thus adversely affecting performance and efficiency.

Heat Transfer in Reciprocating Systems

Unsteady heat transfer in reciprocating systems (engines, compressors, expanders, etc.) has been the subject of various investigations [30-36]. These have shown that it is not possible to describe the convective heat transfer process with a single, constant heat transfer coefficient. In fact, the employment of such a "steady flow" heat transfer coefficient in the quantitative description of the unsteady thermal interaction between a solid and fluid, although a simple and powerful approach can be seriously inadequate in many cases. Yet, many theoretical and modelling approaches assume a constant value for the heat transfer coefficient taken from steady flows in order to quantify the unsteady convective heat exchange. In other studies tempts are made to modify the Nusselt number correlations generated in steady flows, through the definition of suitable Reynolds numbers, and have shown that this goes some way towards offering a correction, but that important deviations remain [37].

Studies that do account for the unsteady heat transfer process often continue to neglect the full, conjugate problem by assuming either a constant temperature or a constant heat flux boundary condition at the (internal) solid-fluid surface. Consequently, computational results are often in considerable disagreement with experiments. The assumption of a constant wall temperature may sometime be adequate when dealing with gases, but this is not always the case (as we will show) and becomes strenuous at best when high heat transfer coefficients are present or under certain geometrical conditions [38].

In this paper a simple, one-dimensional framework is presented that has been developed for the quantitative description of unsteady and conjugate heat transfer in the presence of displacement work. This framework applies the approach presented in Ref. [38,39] to a generalised model of a reciprocating compression and/or expansion process. The specific process that will be examined is that of a gas spring, in which a fixed mass undergoes sequential compression and expansion within the same close space (volume) [30,32,33,36].

METHODS

Problem Formulation

The full problem treated here deals with the thermodynamic process undergone by a fixed mass of gas trapped in a reciprocating piston-in-cylinder configuration in the presence of finite heat transfer from/to the gas, with a fixed temperature imposed on the *external* (rather than the internal) wall of the cylinder. The latter has been done in order to estimate the effects of conjugate heat transfer. This is also an approximation, but one that allows assessment of the thermal properties of the wall. The model that is developed is valid for operation at low volumetric compression ratios ($1 < C_R < 6$), due to the description used for the convective heat transfer coefficient in the fluid, however, this can be easily extended to higher compression ratios C_R. Radiative heat transfer, mechanical and fluid viscous losses are not considered.

Consider the sinusoidal compression and expansion with frequency ω_1 of a mass of gas m enclosed by the cylinder and the reciprocating piston shown in Figure 1.

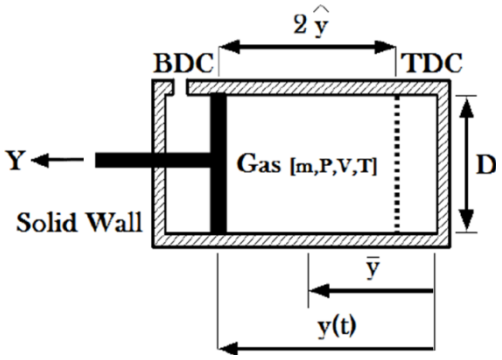

Figure 1 Schematic of the gas spring problem

The geometry features a piston of diameter D following an *imposed* reciprocating motion (e.g., by connection via a mechanism to a motor rotating at constant angular speed ω_1), with amplitude $\hat{y}$ about a mean position $\overline{y}$ described by:

$$y(t) = \overline{y} + \hat{y}\cos(\omega_1 t) \qquad (1)$$

During a cycle the piston makes one full movement from bottom dead centre (BDC) to top dead centre (TDC) and back again. As the piston progresses from BDC to TDC the volume enclosed by the piston $V(t) = Ay(t)$ decreases, which results in a corresponding increase in the pressure $P(t)$ and temperature $T_f(t)$ of the enclosed gas. Here, $A = \pi D^2/4$ is the cross-sectional area of the cylinder. Conversely, as the piston travels back to BDC the pressure P and temperature of the gas T_f will decrease. It is assumed that the mass of gas enclosed by the spring m is fixed, i.e. there is no leakage between the piston and the cylinder, and that the gas is ideal.

The fluctuations in the fluid temperature $T_f(t)$ during the cycle give rise to time-varying heat transfer between the fluid and the walls of the cylinder $\dot{Q}_f(t)$, and consequently also, through the cylinder walls to the environment, which is assumed to be isothermal at *constant* (external) temperature T_0. In general, the solid wall temperature $T_w(t)$ will be fluctuating in response to the time-varying heat transfer rate $\dot{Q}_f(t)$.

Following Lee [30], Kornhauser and Smith [32,33] and others, cyclic convective heat transfer in a gas spring may be described by Newton's law of cooling while employing complex temperatures, heat fluxes and Nusselt numbers Nu. This results in a complex formulation of Newton's law:

$$\dot{q}_f = \frac{k_f}{D}\left[Nu_{\Re}(T_f - T_w) + Nu_{\Im}\frac{1}{\omega_1}\frac{d(T_f - T_w)}{dt}\right] \qquad (2)$$

Note that in Eq. (2), $\dot{q}_f$ is a flux, i.e. the heat transfer rate $\dot{Q}_f(t)$ per unit *time-varying* surface area available to heat transfer

$S(t)$, which includes the sides of the cylinder, as well as its base and the face of piston, such that $S(t) = \pi D y(t) + \pi D^2/2$. In addition, and contrary to convention, note that $\dot{q}_\mathrm{f}$ is defined as *positive* when *leaving* the gas (see also Eqs. (9) and (21)).

The imaginary part of the complex Nusselt number formulation in Eq. (2) arises physically from a turning point in the temperature profile through the gas [40], caused by the work done by/on the gas, which acts to introduce a phase difference between the heat flux at the wall $\dot{q}_\mathrm{f}$ and the bulk temperature difference across the gas $T_\mathrm{f} - T_\mathrm{w}$.

For Pe_ω < 100, the Nusselt number Nu was derived by solving the energy equation in the gas after simplification [30]:

$$Nu = Nu_\Re + \mathrm{i}.\, Nu_\Im = \sqrt{2Pe_\omega}\, \frac{(1+i)\tanh z}{1-\tanh z/z} \tag{3}$$

which is a function of the Péclet number Pe_ω,

$$Pe_\omega = \frac{\omega D^2}{4\alpha_{\mathrm{f},0}} \tag{4}$$

and where $z = (1+i)\sqrt{Pe_\omega/8}$.

For Pe_ω > 100, the Nusselt number Nu was taken from a correlation derived empirically by Kornhauser and Smith [33]:

$$Nu_\Re = Nu_\Im = 0.56\, Pe_\omega^{0.69} \tag{5}$$

The complex Nusselt number Nu relationships are shown together in Fig. 2 as a function of the Péclet number Pe_ω.

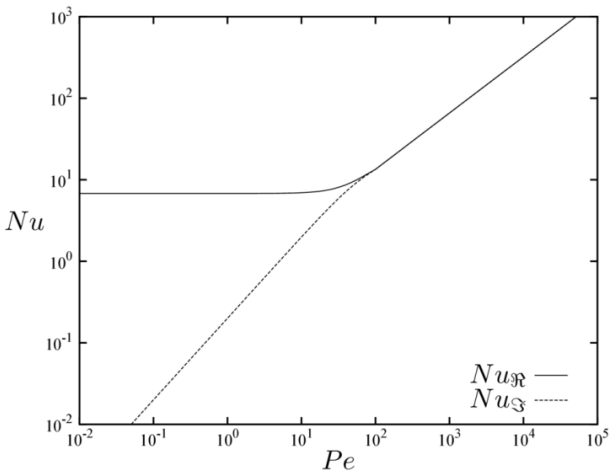

Figure 2 Imposed complex Nusselt number Nu as a function of Péclet number Pe_ω from Refs. [30,33]

The heat flux through the wall $\dot{q}_w$ can be found as the cyclic convolution (operation denoted by '*') of the solid's thermal response to fluctuations in the wall temperature [38,39]:

$$\dot{q}_w = (T_w - T_0) * \frac{1}{Z} \tag{6}$$

where the thermal response, or "impedance" of the solid for an isothermal outer boundary condition $Z_n = Z(\omega_n)$ at a given frequency ω_n can be found by solving the one-dimensional unsteady heat diffusion equation in the solid [38,39]:

$$Z_n = \frac{(1-i)}{2}\frac{\delta_{\mathrm{s},n}}{\kappa_\mathrm{r}} \tanh\left\{(1+i)\frac{a}{\delta_{\mathrm{s},n}}\right\} \tag{7}$$

which contains a thermal diffusion lengthscale in the solid, sometimes referred to as the "thermal penetration depth":

$$\delta_{\mathrm{s},n} = \sqrt{\frac{2k_\mathrm{s}}{\rho_\mathrm{s} c_\mathrm{s} \omega_n}} \tag{8}$$

and where a is the thickness of the cylinder wall, $\kappa_\mathrm{r} = k_\mathrm{s}/k_\mathrm{f}$ is a solid to fluid thermal conductivity ratio, and, ρ_s and c_s are the solid density and specific heat capacity.

Equations (2) and (6) can be solved for T_w since $\dot{q}_\mathrm{f} = \dot{q}_\mathrm{w}$, while integrating the energy equation (i.e., Eq. (9)) to solve for the evolution of the bulk fluid temperature $T_\mathrm{f}(t)$ over the cycle:

$$mc_v dT_\mathrm{f} + A\dot{q}dt + \rho R T_\mathrm{f} dV = 0 \tag{9}$$

Performing dimensional analysis on the above equations it can be seen that the system can be described by 9 independent variables. The set of chosen variables is shown below:

$$f\left\{\begin{array}{c} R_\mathrm{SB} = \frac{\overline{y}}{D}, y_\mathrm{a} = \frac{\hat{y}}{\overline{y}}, b_\mathrm{s} = \frac{a}{\delta_{s,1}}, \\ \kappa_\mathrm{r} = \frac{k_\mathrm{s}}{k_\mathrm{f}}, \rho_{\mathrm{r},0} = \frac{\rho_\mathrm{s}}{\rho_{\mathrm{f},0}}, c_\mathrm{r} = \frac{c_\mathrm{s}}{c_v}, \gamma, \\ Pe_\omega = \frac{\omega_1 D^2}{4\alpha_{\mathrm{f},0}}, T_0^* = \frac{c_v T_0}{\frac{1}{2}(\omega_1 D)^2} \end{array}\right\} \tag{10}$$

where $\rho_{\mathrm{f},0}$ and $\alpha_{\mathrm{f},0}$ are the density and thermal diffusivity of the gas phase when the piston is in the mean (central) position, $y(t) = \overline{y}$. The variables include: (i) ratios of geometric parameters, and of fluid and solid thermophysical properties; (ii) the Péclet number Pe_ω; and (iii) a dimensionless external (environment) temperature T_0^*, with T_0 constant.

The dimensionless geometric parameters that describe the geometry of the gas spring are found by normalising against each variable's mean value, giving the displacement (y^*), area (A^*), volume (V^*) and density (ρ^*) variables given below:

$$y^* = \frac{y}{\overline{y}} = 1 + y_\mathrm{a} \sin(\omega^* t^*) \tag{11}$$

$$A^* = \frac{2y^* R_\mathrm{SB} + 1}{2R_\mathrm{SB} + 1} \tag{12}$$

$$V^* = \frac{V}{\overline{V}} = y^* \tag{13}$$

$$\rho^* = \frac{\rho_\mathrm{f}}{\rho_{\mathrm{f},0}} = \frac{1}{V^*} \tag{14}$$

where $t^* = \omega_1 t$ is the dimensionless time and $\omega^* = 1$ the dimensionless harmonic frequency.

Normalising all temperatures by $(\omega_1 D)^2/2c_v$, which is a measure of the amount of energy given to the system scaled as a temperature, results in the dimensionless temperature:

$$T^* = \frac{c_v T}{\frac{1}{2}(\omega_1 D)^2} \tag{15}$$

and the dimensionless pressure:

$$P^* = P\frac{c_v}{\frac{1}{2}(\omega_1 D)^2 \rho_{\mathrm{f},0} R} = \rho^* R^* T_\mathrm{f}^* \tag{16}$$

Accordingly, the *real part* of the heat flux $\dot{q} = \dot{q}_\mathrm{f} = \dot{q}_\mathrm{w}$ in Eq. (2) becomes:

$$\dot{q}^* = \dot{q}\frac{c_v}{\frac{1}{2}(\omega_1 D)^2}\frac{D}{k_f} = Nu_{\Re}(T_f^* - T_w^*) + Nu_{\Im}\frac{d(T_f^* - T_w^*)}{dt^*} \quad (17)$$

and Eq. (6) is re-written as:

$$\dot{q}^* = (T_w^* - T_0^*) * \frac{1}{Z^*} \quad (18)$$

where Z^* is the dimensionless thermal impedance of the solid at a given dimensionless frequency S_n^*, such that:

$$Z^* = Z\frac{k_f}{D} = \frac{(1-i)}{2\kappa_r}\sqrt{\frac{\alpha_{r,0}}{2\,Pe_\omega\,S_n^*}}\tanh\left\{(1+i)\frac{a}{\delta_{s,n}}\right\} \quad (19)$$

whereby the dimensionless frequency is defined as $S_n^* = \omega_n/\omega_1 = n$. Furthermore:

$$\alpha_{r,0} = \frac{\kappa_r\gamma}{\rho_{r,0}c_r} = \left(\frac{\delta_{s,1}}{\delta_{f,0}}\right)^2 \quad (20)$$

in Eq. (19) is the solid to fluid thermal diffusivity ratio, with the former evaluated at the fundamental frequency ω_1 and the latter evaluated when the piston is in the central position $y(t) = \overline{y}$.

Finally, Eq. (9) that describes the energy balance in the gas domain becomes:

$$\frac{1}{\gamma-1}dT_f^* + \frac{\gamma}{\gamma-1}\frac{(2+R_{SB}{}^{-1})}{2Pe_\omega}A^*\dot{q}^*dt^* + \rho^*R^*T_f^*dV^* = 0 \quad (21)$$

On examination of Eq. (21) it is observed that for low Péclet numbers Pe_ω the majority of the work done by the gas will be exchanged in the form of heat with the solid walls, and the system will effectively undergo isothermal compression and expansion. On the other hand, at high Péclet numbers Pe_ω the heat exchanged will be minimal, and the system will experience adiabatic compression and expansion.

Consequently, we would expect that at intermediate Péclet numbers Pe_ω the work will result from an interplay between both the internal energy of the gas and the heat transfer to the solid and, by extension, the environment. A phase lag between the temperature of the fluid T_f^* and the heat transfer $\dot{q}^*$ will result in a net loss of work around the cycle.

A useful metric to gauge the relative importance of the fluid and solid domains in the heat transfer solution is the Biot number, which can be interpreted as a ratio of temperature changes in the fluid to temperature changes across the solid:

$$Bi = Nu_{\Re}b_s\frac{1}{\sqrt{2\epsilon_r Pe_\omega}} \quad (22)$$

By definition the solution to the gas spring problem will deviate from the isothermal boundary condition imposed in all previous studies on the internal walls of the cylinder when the Biot number Bi is large. In this condition the temperature of the wall will begin to fluctuate. Due to the relationship of $Nu_{\Re}$ to the Péclet number Pe_ω, the Biot number Bi will become large when the Péclet number is either much less than one $Pe_\omega \ll 1$ or much greater than one $Pe_\omega \gg 1$. Two additional parameters of importance in determining the Biot number Bi are the effusivity ratio $\epsilon_r = \kappa_r\rho_{r,0}c_r\gamma$ between the solid and the fluid, and the ratio b_s of the wall thickness to the thermal diffusion length in the solid. Both small effusivity ratios ϵ_r and/or large lengthscale ratios b_s lead to large Biot numbers Bi.

RESULTS AND DISCUSSION

Cyclic heat flux and temperature differences in the fluid

Figure 3 shows typical temperature difference-heat flux (θ-$\dot{q}$) plots for two gas spring cases: (a) Pe_ω = 17 and $a/\delta_{s,1}$ = 3.2×10^{-1}; and (b) Pe_ω = 1000 and $a/\delta_{s,1}$ = 1.9. The temperature difference refers to the difference between the fluid and the internal surface of the solid wall:

$$\theta_{f,w} = T_f - T_w \quad (23)$$

In a (quasi-) steady scenario one would expect to see straight lines passing through the origin without hysteresis; that is with a gradient that is not dependent on the direction of the process (i.e., heating *vs*. cooling). The closed area inscribed by the resulting curves is an indicator of the (imposed, through Eqs. (2) to (5)) phase difference between θ and $\dot{q}$.

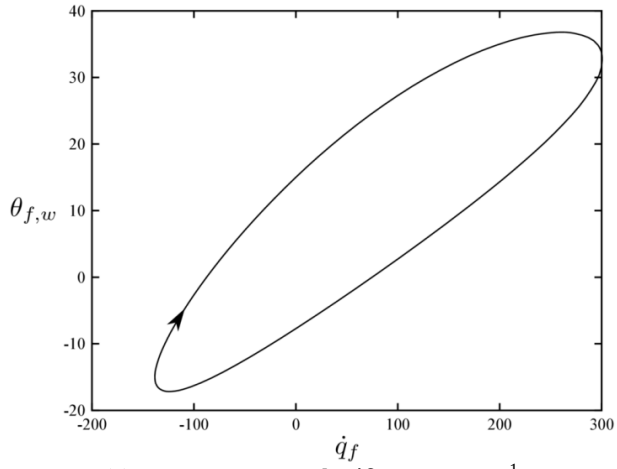

(a) For Pe_ω = 17 and $a/\delta_{s,1}$ = 3.2×10^{-1}

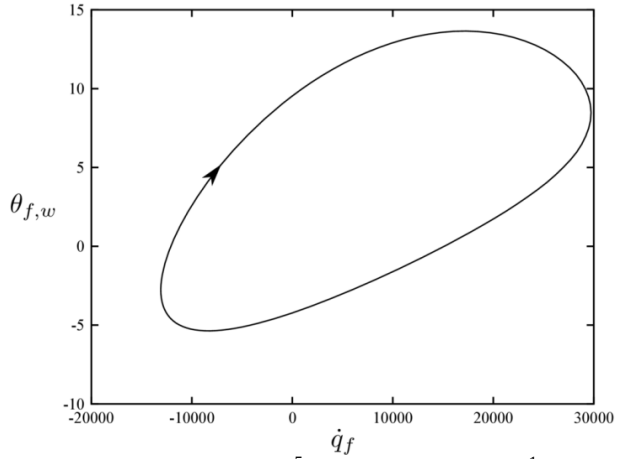

(b) For Pe_ω = 1×10^5 and $a/\delta_{s,1}$ = 3.2×10^{-1}

Figure 3 Modelled heat flux $\dot{q}$ and temperature difference θ around the cycle for a gas spring with κ_r = 1, $\rho_{r,0}$ = 1 and c_r = 1

Moreover, a *positive asymmetry* of this plot with respect to the vertical axis at $\dot{q}$ = 0, would suggest a net heat flow from the gas to the solid, and hence also from the solid to the surroundings, which can only come from a net work *input* to the gas spring cycle. This work input is a pure loss, with the

ideal gas spring requiring exactly the same amount of work to compress the gas as is gained by its subsequent expansion.

Time-varying heat transfer coefficient

It is useful to be able to evaluate the expected value of the heat transfer coefficient h in thermodynamic processes such as the one presented in this paper, so as to characterise the heat transfer performance. The heat transfer coefficient, $h = \dot{q}/\theta$, is a ratio of two variables which, in these problems, fluctuate about zero; namely the heat flux $\dot{q}$ and the temperature difference across the fluid $\theta = T_\mathrm{f} - T_\mathrm{w}$. This results in a heat transfer coefficient h which has a probability distribution that can be approximated by a Cauchy distribution function:

$$P_\mathrm{C}(h) = \frac{1}{\pi\xi\left[1+\left(\frac{h-h_0}{\xi}\right)^2\right]} \quad (24)$$

where h_0 is the location parameter, or expected value of h, describing the location of the peak probability density and ξ is the scale, or width, of the distribution. Such a distribution will arise, for example, if the two independent variables (heat flux $\dot{q}$ and temperature difference θ) are normally distributed. It can be seen from Fig. 4 that the Cauchy distribution fits the modelled Nusselt number Nu remarkably well, providing a level of confidence in this choice of distribution function.

It is important to note that a Cauchy distribution has no defined mean value or higher moments. Additionally, when using numerical methods or experimental data the mean is evaluated using a sample mean estimator which, for a Cauchy distribution, is itself a Cauchy distribution. Furthermore even if expressions for $\dot{q}$ and θ are known analytically, the mean value of the heat transfer coefficient h cannot be calculated since the integral for the expected value of h will not converge. Therefore the mean value of the Nusselt number $\overline{Nu}$ (and consequently also, of $\overline{h}$) cannot be used to estimate the expected value, and a sample mean will give unpredictable results. Despite this limitation, the parameters h_0 and ξ can be estimated by maximising the log likelihood estimator:

$$l\left(h_0,\xi \mid h_1, h_2, \ldots h_n\right) = n\left[\log(\xi) - \log(\pi)\right] - \sum_{i=1}^{n}\log(\xi + (h_i - h_0)^2) \quad (25)$$

This estimation is performed herein in order to provide a value for the expected values of the heat transfer coefficient h_0 and a corresponding value for the Nusselt number $Nu_{h,0}$.

Case 1: Unity material property ratios

We now proceed to investigate the gas spring case with the three key material property ratios set to unity, that is, with κ_r = 1, $\rho_{\mathrm{r},0}$ = 1 and c_r = 1. The main results are shown in Fig. 5.

The work loss ψ due to heat transfer in Fig. 5a is defined as:

$$\psi = \frac{\oint W dt}{\oint |W| dt} \quad (26)$$

in accordance with the earlier discussion concerning this parasitic net work input to the thermodynamic cycle. Also, recall that in the present model no account is made for losses due to turbulence or viscous dissipation in the fluid.

Considering the case when the wall thickness is small, i.e., $a/\delta_{s,1}$ = 0.01 in Fig. 5a, the thinness of the wall gives rise to a strong coupling of the internal surface of the solid wall to the external (isothermal) boundary condition T_0, which in turn results in the internal wall-fluid boundary condition being effectively isothermal. This is the condition that has been solved by Lee [30], and almost all other similar studies.

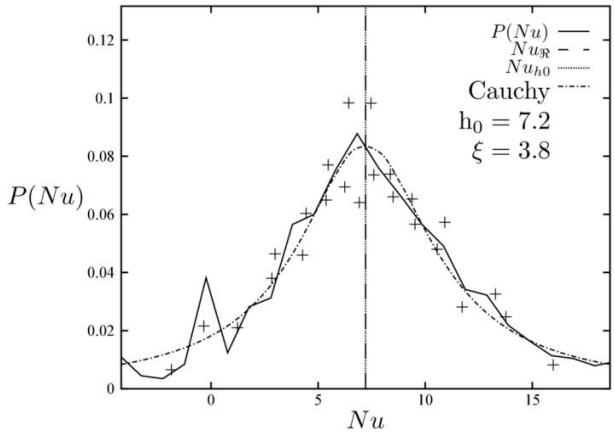

(a) Distribution of Nu for Pe_ω = 17 and $a/\delta_{s,1} = 3.2\times10^{-1}$, showing a Cauchy approximation with expected value $Nu_{h,0} \approx Nu_\Re$ = 7.2 and ξ = 3.8

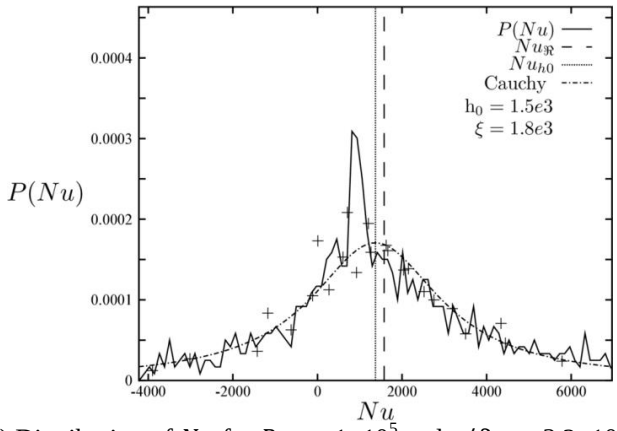

(b) Distribution of Nu for $Pe_\omega = 1\times10^5$ and $a/\delta_{s,1} = 3.2\times10^{-1}$, showing a Cauchy approximation with expected value $Nu_{h,0}$ = 1.5×10^3 and $\xi = 1.8\times10^3$.4

Figure 4 Distribution of the instantaneous Nusselt number Nu and Cauchy approximations $P_\mathrm{C}(Nu)$

At low Péclet numbers Pe_ω the frequency is low enough to allow heat transfer to take place between the fluid contained within the spring and the solid walls of the cylinder and piston, thus allowing the fluid to remain at (or near) thermal equilibrium with the solid. As such, the gas effectively experiences isothermal compression and expansion. In this condition all of the work done on the gas is transferred as heat to the walls but across a very small temperature difference, resulting in a low cycle loss. Similarly, at high Péclet numbers Pe_ω the process is fast enough not to allow sufficient time for heat exchange. In these conditions the system is, in effect, undergoing adiabatic compression and expansion with the majority of the work being exchanged with the internal energy

of the gas. The thermal cycle loss is again low.

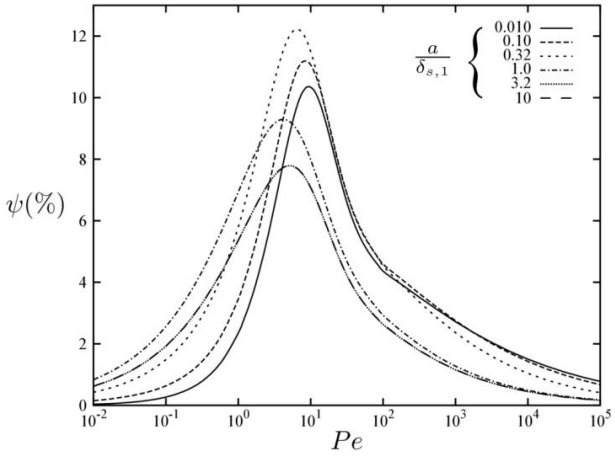

(a) Thermal cycle loss ψ in % points, from Eq. (26)

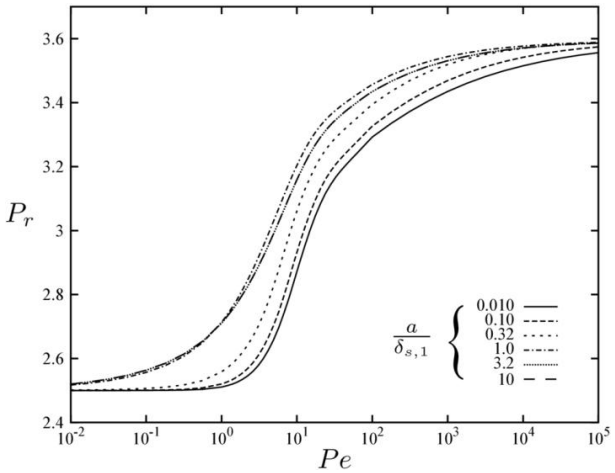

(b) Pressure ratio $Pr = \min\{P\}/\max\{P\}$

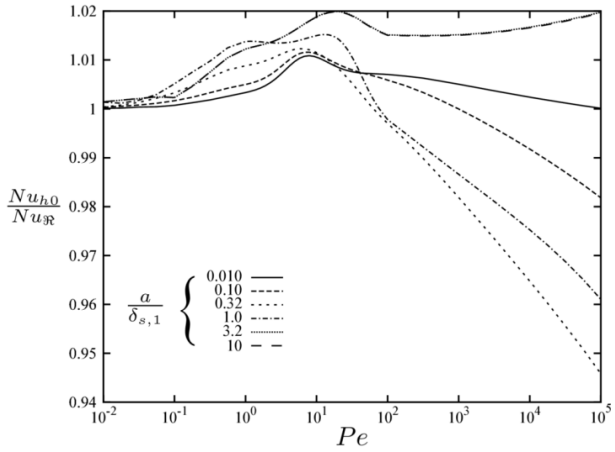

(c) Expected Nusselt number $Nu_{h,0}$

Figure 5 Response of a gas spring with the material ratios $\kappa_r = 1$, $\rho_{r,0} = 1$ and $c_r = 1$ as a function of Péclet number Pe_ω and for different $a/\delta_{s,1}$ from 0.010 to 10

When the Péclet number Pe_ω is at an intermediate value, however, heat is exchanged out of phase with the (finite) temperature difference θ across the gas resulting in an exegetic cycle loss. From Fig. 5a, the peak thermal loss with an isothermal external wall boundary condition is about 10% and occurs at a Péclet number Pe_ω of around 10. This compares well to the result from Lee [30], though the loss here appears shifted to a slightly higher Pe_ω due to the fact that in the present work a volumetric variation is imposed on the gas (Eq. (1)), whereas in Lee [30] (and elsewhere) a pressure variation is imposed with a given pressure ratio. This is associated with higher pressure ratios at higher Pe_ω, as demonstrated in Fig. 5b, where it shown that as the system moves from isothermal (low Pe_ω) to adiabatic (high Pe_ω) operation the pressure ratio for the same volumetric time-variation increases.

In the case of having a thick wall with $a/\delta_{s,1}$ = 10 it is observed that the internal wall condition is only weekly coupled to (insulated from) the external boundary condition, and so the temperature at the interface between the wall T_w and fluid temperatures T_f are free to fluctuate. At high Péclet numbers Pe_ω the effect of the thicker cylinder wall is to make the system more adiabatic and to reduce the thermal losses. Nevertheless, at lower Pe_ω the effect of the finite fluctuations in wall temperature T_w act so as to move the cycle away from the ideal isothermal process, leading to higher thermal losses. This is somewhat counter-intuitive: one would expect the addition of material to have an insulating effect and to reduce the thermal loss, through an increase in the thermal resistance due to conduction. In fact, the peak thermal loss has reduced, and the peak has migrated to a lower value of Pe_ω.

When the wall thickness is chosen to be of order unity, or that $a/\delta_{s,1} \sim \mathcal{O}(1)$, the magnitude of the thermal loss is greater than that observed at both low and high $a/\delta_{s,1}$. This arises from a thermal interaction in the solid (in the unsteady conduction) between the internal and external walls and leads to a modification of the phase of the heat flux out of the fluid $\dot{q}_f$. Thus, even though the *magnitude* of the heat flux $\dot{q}_f$ is reduced, the phase at which it occurs relative to the temperature across the fluid θ gives rise to a greater cycle loss.

Case 2: Conventional material properties

The ratios of material properties in conventional systems do not typically equal unity, with the solid walls of the piston and cylinder likely to be considerably denser than the gas. The thermal conductivity of the solid is also likely to be higher, though the specific heat capacities of many gases tend to be higher than that of common solids. We consider a set of more typical values for our selected solid and gas properties by imagining that the walls of the cylinder are coated in a plastic such as PTFE or acrylic, and that the spring is filled (when extended to BDC) with hydrogen at 50 bar at 300 K. The material ratios become κ_r = 1.06, $\rho_{r,0}$ = 145.1 and c_r = 0.15.

In this case the effect of the wall (see Fig. 6) is very much reduced compared to our earlier results in Fig. 5. Nevertheless, the exergetic loss exhibits similar characteristics to those observed previously, according to which $a/\delta_{s,1} \sim \mathcal{O}(1)$ produces the maximum loss and thicker walls makes the fluid boundary condition less isothermal, increasing the cycle losses at low Péclet numbers Pe_ω and reducing them at high ones.

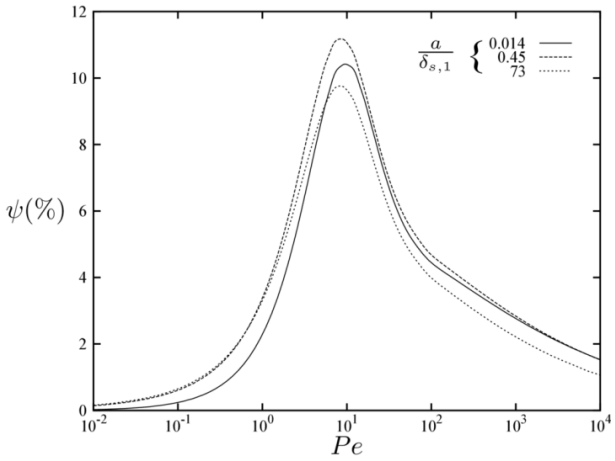

Figure 6 Thermal cycle loss ψ in a gas spring (in % points) as a function of Péclet number Pe_ω, with the material property ratios set to κ_r = 1.06, $\rho_{r,0}$ = 145.1 and c_r = 0.15, and over a range of wall thicknesses a/δ

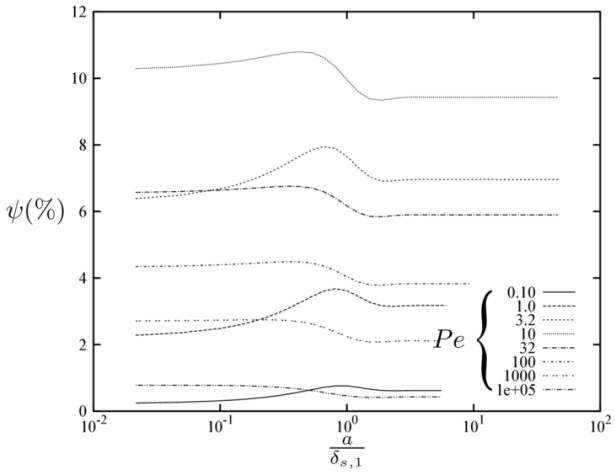

Figure 7 Thermal cycle loss ψ in a gas spring (in % points) as a function of dimensionless wall thickness a/δ, with the material property ratios set to κ_r = 1.06, $\rho_{r,0}$ = 145.1 and c_r = 0.15, and over a range of Péclet numbers Pe_ω

Figure 7 shows more clearly the dependence of the irreversible thermal loss on the dimensionless wall thickness $a/\delta_{s,1}$. A wall thickness exists for which the maximum loss arises for a given Péclet number Pe_ω. The shape of these plots leads to a non-trivial conclusion with significant implications. Starting from a thin wall, it is interesting to observe that increasing the thickness of the wall, or insulation, is expected to lead to *higher* cycle losses, after which the losses decrease again. At low Pe_ω the loss reduction at the highest $a/\delta_{s,1}$ does not return the overall loss to its minimum value observed at the lowest $a/\delta_{s,1}$, as opposed to the higher values of $Pe_\omega > 5$.

By comparing the wall heat flux $\dot{q}^*$ from Eqs. (17) and (18) it can be seen that:

$$\dot{q}^* \sim \frac{\theta_{w,0}}{Z^*} \sim Nu\ \theta_{f,w} \tag{27}$$

where $\theta_{j,k} = T_j^* - T_k^*$ is the temperature difference across the solid or fluid domain. Due to the way in which Z^* scales with a/δ_s in Eq. (19), and specifically given that $\tanh\{x\} \sim x$ for $x \ll 1$, Eq. (27) leads to a scaling for the ratio of the temperature difference across the fluid to the temperature difference across the solid domain, $\theta_{w,0}/\theta_{f,w}$, of the form:

$$\frac{\theta_{w,0}}{\theta_{f,w}} \sim \frac{Nu}{\sqrt{2\epsilon_r Pe_\omega}} \frac{a}{\delta_s} = Bi \tag{28}$$

when a/δ_s is less than one. Eq. (28) also applies to the steady state (mean temperature difference) part of the solution, since the steady state problem is associated with an a/δ_s of zero. When a/δ_s is greater than one the ratio of the fluctuations in the temperature differences across the domains will still scale with Bi, but with a modification due to $\tanh\{x\} \sim 1$ for $x \gg 1$:

$$\frac{\theta_{w,0}}{\theta_{f,w}} \sim \frac{Nu}{\sqrt{2\epsilon_r Pe_\omega}} = Bu = \frac{Bi}{\frac{a}{\delta_s}} \tag{29}$$

where Bu is an "unsteady" Biot number.

Expressions (28) and (29) show the relative importance of the solid to the fluid domain on the solution, and are essentially a function of the Péclet number Pe_ω and the material thermal effusivity ratio ϵ_r (since the Nusselt number Nu is also a function of the Péclet number Pe_ω). When the Biot Bi or unsteady Biot Bu numbers are less than one the fluctuations of the wall temperature T_w^* are minimal and the problem is equivalent to having an isothermal wall temperature. Conversely when the Bi or Bu numbers are greater than one the wall temperature T_w^* will fluctuate significantly, thus affecting the solution. It can be seen therefore that the solid walls of the gas spring cylinder do affect the cycle undertaken by the gas when the effusivity ratio ϵ_r between the solid and the gas is low. In Fig. 6 the effusivity ratio was ϵ_r = 32.3, whereas in Fig. 5 this was ϵ_r = 1.40. As expected, at lower ratios ϵ_r the walls of the cylinder have a greater effect on the cycle losses.

Case 3: Materials with unfavourable properties

The gas spring can exhibit more extreme effects due to the solid wall when the effusivity ratio ϵ_r is lowered below unity. To obtain a low effusivity the heat capacity, thermal conductivity and density of the gas must be high relative to the solid. Hydrogen has the highest specific heat capacity c_v and thermal conductivity k_f of any gas. Gases with higher atomic weights have higher densities ρ_f for the same pressure, however, this is outweighed by their lower heat capacities c_v and lower thermal conductivities k_f, thus leading to lower thermal effusivities ϵ. In addition, if turbulence is introduced into the gas spring chamber, such as would expected when operating with a gas intake and exhaust through suitable valves, Cantelmi [34] showed that this can be modelled by a modified "turbulent" thermal conductivity for the gas which can be up to 30 times larger than the non-turbulent (molecular) case. Finally, if the cylinder walls are made of a low density material, such as a foam, the thermal conductivity k_s, heat capacity c_s and density ρ_s of the solid side are also significantly reduced.

Using hydrogen gas at high pressure, specifically ~100 bar, an equivalent turbulent thermal conductivity multiplier guided by and with a foam layer insulating the inside of the cylinder Cantelmi [34] and a cylinder and piston faces with internal

surfaces insulated by a foam (this can be fitted within a metal outer section for structural strength) it is feasible to obtain material ratios of κ_r = 0.033, $\rho_{r,0}$ = 10 and c_r = 0.07, which correspond to a thermal effusivity ratio of ϵ_r = 0.032. The results for the work loss ψ obtained from the gas spring described in the above paragraphs above are shown in Fig. 8. Clearly the losses are more pronounced in this case, reaching a maximum value of up to 14% at intermediate dimensionless wall thickness $a/\delta_{s,1}$ and Péclet number Pe_ω values.

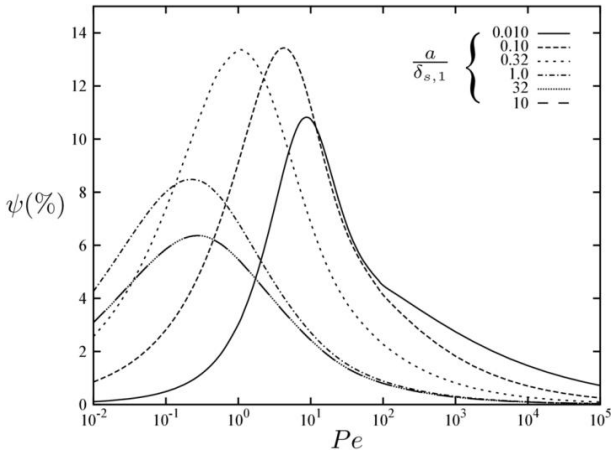

Figure 8 Thermal cycle loss ψ in a gas spring (in % points) as a function of Péclet number Pe_ω, with the material property ratios set to κ_r = 0.033, $\rho_{r,0}$ = 10 and c_r = 0.07, and over a range of wall thicknesses $a/\delta_{s,1}$

Finally, an interesting feature can also be seen in Fig. 9, where the pressure ratio Pr is higher at a intermediate wall thicknesses $a/\delta_{s,1} \sim O(1)$ compared to when the wall is much thicker than the diffusion length $\delta_{s,1}$. It is noted from that the loss gives rise to a requirement for a larger pressure ratio Pr to drive the same volumetric compression of the gas.

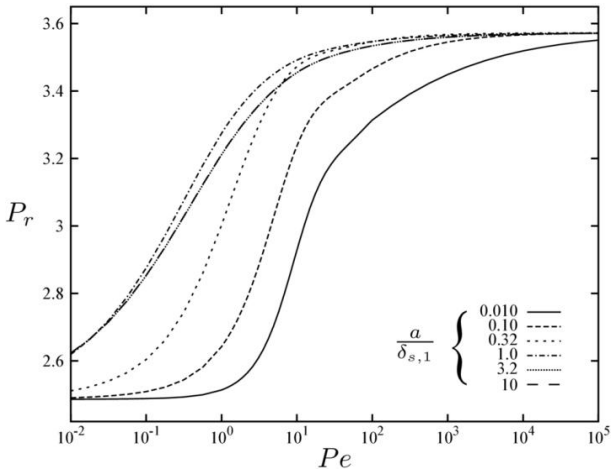

Figure 9 Pressure ratio Pr in a gas spring as a function of Péclet number Pe_ω, with the material property ratios set to κ_r = 0.033, $\rho_{r,0}$ = 10 and c_r = 0.07, and over a range of wall thicknesses $a/\delta_{s,1}$

CONCLUSIONS

A conjugate model that solves the one-dimensional unsteady heat conduction equation in the solid simultaneously with the first law in the gas phase has been applied to the study of gas springs. An imposed heat transfer coefficient has been used, which was taken from relevant experimental studies in the literature. Beyond the explicit inclusion of conjugate heat transfer, the model goes beyond previous investigations by considering the case of imposed volumetric compression and by allowing the resulting gas pressure to vary accordingly.

Notable effects of the solid walls of the gas spring are uncovered, with worst case cycle losses due to irreversible heat transfer of up to about 14% for cases in which unfavourable materials (solid/gas) are selected, and closer to 11% for more common material choices. The contribution of the solid itself through the cylinder wall thickness accounted for about 8% and 2% of the total loss, respectively. These results suggest that, in designing high-efficiency compression and expansion machines but also similar thermo-mechanical systems, the full conjugate and unsteady problem must be considered if an accurate prediction of potential performance is to be obtained.

REFERENCES

[1] Backhaus S., and Swift G.W., A thermoacoustic-Stirling heat engine: Detailed study, *Journal of the Acoustical Society of America*, Vol. 107, 2000, pp. 3148-3166

[2] Wheatley J., Hofler T., Swift G.W., and Migliori A., An intrinsically irreversible thermoacoustic heat engine, *Journal of the Acoustical Society of America*, Vol. 74, 1983, pp. 153-170

[3] Ceperley P.H., A pistonless Stirling engine–The travelling wave heat engine, *Journal of the Acoustical Society of America*, Vol. 66, 1979, pp. 1508-1513

[4] West C.D., and Pandey R.B., Laboratory prototype Fluidyne water pump, Proceedings of the 16th Intersociety energy conversion Engineering Conference, Atlanta, GA, USA, 9-14 August, 1981, pp. 1916-1918

[5] West C.D., Dynamic analysis of the Fluidyne, *Proceedings of the 18th* Intersociety *Energy Conversion Engineering Conference*, Orlando, FL, USA, 21-26 August, 1983, pp. 779-784

[6] Stammers C.W., The operation of the Fluidyne heat engine at low differential temperatures, *Journal of Sound and Vibration*, Vol. 63, 1979, pp. 507-516

[7] Markides C.N., and Smith T.C.B., A dynamic model for the efficiency optimization of an oscillatory low grade heat engine, *Energy*, Vol. 36, 2011, pp. 6967-6980

[8] Solanki R., Galindo A., and Markides C.N., Dynamic modelling of a two-phase thermofluidic oscillator for efficient low grade heat utilization: Effect of fluid inertia, *Applied Energy*, Vol. 89, 2012, pp. 156-163

[9] Solanki R., Galindo A., and Markides C.N., The role of heat exchange on the behaviour of an oscillatory two-phase low-grade heat engine, *Applied Thermal Engineering*, *in press*

[10] Redlich R.W., and Berchowitz D.M., Linear dynamics of free-piston Stirling engines, *Proceedings of the Institution of Mechanical Engineers, Part A: Journal of Power and Energy*, Vol. 199, 1985, pp. 203-213

[11] Walker G., and Senft J.R., Free piston Stirling engines, Springer, Berlin, 1985
[12] Wood J.G., and Lane N.W., Advanced 35 We Stirling engine for space power applications, *Proceedings of the space technology and applications International Forum*, Albuquerque, NM, USA, 2-5 February, 2003, pp. 662-667
[13] Huang B.J., and Chuang M.D., System design of orifice pulse-tube refrigerator using linear flow network analysis, *Cryogenics*, Vol. 36, 1996, pp. 889-902
[14] Kentfield J.A.C., Fundamentals of idealized airbreathing pulse-detonation engines, *Journal of Propulsion and Power*, Vol. 18, 2002, pp. 78-83
[15] Organ A.J., Stirling and pulse-tube cryo-coolers, John Wiley and Sons, Bury St. Edmunds, 2005
[16] Mobarak A., Rafat N., and Saad M., Turbine selection for a small capacity solar-powered generator, *Solar Energy: International Progress Proceedings of the International Symposium–Workshop on Solar Energy*, Cairo, Egypt, Vol. 3, 16-22 June, 1978, pp. 1351-1367
[17] Mago P.J., Srinivasan K.K., Chamra L.M., and Somayaji C., An examination of exergy destruction in organic Rankine cycles, *International Journal of Energy Research*, Vol. 32, 2008, 926-938
[18] Badr O., O'Callaghan P.W., Hussein M., and Probert S.D., Multi-vane expanders as prime movers for low-grade energy organic Rankine-cycle engines, *Applied Energy*, Vol. 16, 1984, pp. 129-146
[19] Leibowitz H., Smith I.K., and Stosic N., Cost effective small scale ORC systems for power recovery from low grade heat sources, *Proceedings of the ASME International Mechanical Engineering Congress and Exposition*, Chicago, IL, USA, 5-10 November, 2006
[20] Wang H., Peterson R.B., and Herron T., Experimental performance of a compliant scroll expander for an organic Rankine cycle, *Proceedings of the Institution of Mechanical Engineers, Part A: Journal of Power and Energy*, Vol. 223, 2009, pp. 863-872
[21] Gao X.J., Li L.S., Zhao Y.Y., and Shu P.C., Research on a scroll expander used for recovering work in a fuel cell, *International Journal of Thermodynamics*, Vol. 7, 2004, pp. 1-8
[22] Peterson R.B., Wang H. and T. Herron, Performance of small-scale regenerative Rankine power cycle employing a scroll expander, *Proceedings of the Institution of Mechanical Engineers, Part A: Journal of Power and Energy*, Vol. 222, 2008, pp. 271-282
[23] Badami M., and Mura M., Preliminary design and controlling strategies of a small-scale wood waste Rankine cycle (RC) with a reciprocating steam engine (SE), *Energy*, Vol. 34, 2009, pp. 1315-1324
[24] Yamamoto T., Furuhata T., Arai N., and Mori K., Design and testing of the organic Rankine cycle, *Energy*, Vol. 26, 2001, pp. 239-251
[25] Curran, H.M., Use of organic working fluids in Rankine engines, *Journal of Energy*, Vol. 5, 1981, pp. 218-223
[26] Balje O.E., A study on design criteria and matching of turbomachines: Part A–Similarity relations and design criteria of turbines. *Transactions of the American Society of Mechanical Engineers, Journal of Engineering for Power*, Vol. 84, 1962, 83-102
[27] Moss R., Roskilly A., and Nanda S., Reciprocating joule-cycle engine for domestic CHP system, *Applied Energy*, Vol. 80, 2005, pp. 169-185
[28] White A.J., Thermodynamic analysis of the reverse Joule–Brayton cycle heat pump for domestic heating, *Applied Energy*, Vol. 86, 2009, pp. 2443-2450
[29] Huff H.-J., and Radermacher R., CO_2 compressor-expander analysis, Report ARTI-21CR/611-10060-01, March 2003
[30] Lee K.P., A simplistic model of cyclic heat transfer in closed spaces, *Proceedings of the 18th Intersociety Energy Conversion Engineering Conference*, Orlando, FL, USA, Paper 839116, 21-26 August, 1983, pp. 720-723
[31] Lawton B., Effect of compression and expansion on instantaneous heat transfer in reciprocating internal combustion engines, *Proceedings of the Institution of Mechanical Engineers, Part A: Journal of Power and Energy*, Vol. 201, 1987, pp. 175-186
[32] Kornhauser A.A., and Smith J.L., The effects of heat transfer on gas spring performance, *Transactions of the American Society of Mechanical Engineers, Journal of Energy Resources Technology*, Vol. 115, 1993, pp. 70-75
[33] Kornhauser A.A., and Smith J.L., Application of a complex Nusselt number to heat transfer during compression and expansion, *Transactions of the American Society of Mechanical Engineers, Journal of Heat Transfer*, Vol. 116, 1994, pp. 536-542
[34] Cantelmi F.J., Gedeon D., and Kornhauser A.A., An analytical model for turbulent compression-driven heat transfer, *Transactions of the American Society of Mechanical Engineers, Journal of Heat Transfer*, Vol. 120, 1998, pp. 617-623
[35] Vignon J.-M., and Mazon D., Modèle de transfert de chaleur periodique en compression-détente pure, *International Journal of Thermal Sciences*, Vol. 38, 1999, pp. 89-97
[36] Catto A.G., and Prata A.T., A numerical study of instantaneous heat transfer during compression and expansion in piston-cylinder geometry, *Numerical Heat Transfer, Part A: Applications*, Vol. 38, 2000, pp. 281-303
[37] Piccolo A., and Pistone G., Estimation of heat transfer coefficients in oscillating flows: The thermoacoustic case, *International Journal of Heat and Mass Transfer*, Vol. 49, 2006, 1631-1642
[38] Mathie R., and Markides C.N., Heat transfer augmentation in unsteady conjugate thermal systems – Part I: Semi-analytical 1-D framework, *International Journal of Heat and Mass Transfer, submitted*
[39] Mathie R., and Markides C., Unsteady 1D thermal conduction in finite solids, and composite bodies, *Proceedings of the 11th UK Heat Transfer Conference*, London, UK, Paper UKHTC-059, 6-8 September, 2009, pp. 1-12
[40] Lawton B., Effect of compression and expansion on instantaneous heat transfer in reciprocating internal combustion engines, *Proceedings of the Institution of Mechanical Engineers, Part A: Journal of Power and Energy*, Vol. 201, 1987, pp. 175-186